Structure and Stability of the $[TCNE]_2^{2-}$ Dimers in Dichloromethane Solution: A Computational Study

Iñigo Garcia-Yoldi,[†] Joel S. Miller,[‡] and Juan J. Novoa*,[†]

Departament de Química Física, Facultat de Química & CERQT, Parc Cientìfic, Universitat de Barcelona, Av. Diagonal, 647, 08028-Barcelona, Spain, and Department of Chemistry, University of Utah, Salt Lake City, Utah 84112-0850

Received: April 25, 2007

The solution behavior of $[TCNE]^{\bullet-}$, which forms long-living π-$[TCNE]_2^{2-}$ dimers, is computationally studied by B3LYP and MCQDPT/CASSCF(2,2) calculations (a multiconfigurational quasi-degenerate perturbative calculation using a CASSCF(2,2) wavefunction, which properly accounts for the dispersion interaction). B3LYP calculations indicate minimum-energy $[TCNE]_2^{2-}$(dichloromethane)$_4$ aggregates, a solvent where π-$[TCNE]_2^{2-}$ dimers are spectroscopically observed. Their existence is attributed to $[TCNE]^{\bullet-}\cdots$solvent interactions that exceed the $[TCNE]^{\bullet-}\cdots[TCNE]^{\bullet-}$ repulsion. The lowest energy minimum at the B3LYP level corresponds to an open-shell singlet electronic structure, a metastable minimum where the shortest interanion C···C distance is 5.23 Å. A slightly less stable minimum is also found for the closed-shell singlet when double-occupancy of the orbitals is imposed, but it converts into the open-shell singlet minimum when the double occupancy is relaxed. At the MCQDPT/CASSCF(2,2) level, the only minimum is for the closed-shell singlet (24.0 kcal/mol (101 kJ/mol) more stable than the dissociation products), consistent with experimental enthalpy of dimerization of $[TCNE]^{\bullet-}$ in dichloromethane solutions. It has an interanion C···C distance of 2.75 Å and is in accord with the UV−vis experimental properties of the $[TCNE]^{\bullet-}$ solutions.

Introduction

Organic species exhibiting unusually long, multicentered CC bonds have been the focus of several recent studies.[1−5] The prototype, $[TCNE]_2^{2-}$ (TCNE = tetracyanoethylene) dimers, forms long (∼2.9 Å) two-electron C−C bonds involving four carbon atoms.[1−3] The bond arises from the overlap of the b_{2g} SOMO $[TCNE]^-$ orbitals to form bonding and antibonding orbitals of b_{2u} and b_{1g} symmetry, respectively, for the $[TCNE]_2^{2-}$ (Figure 1), and exhibits the same electronic properties as conventional covalent chemical bonds. To date 17 crystallographically determined structures possessing $[TCNE]_2^{2-}$ have been reported, and the intradimer C−C separation is 2.89 ± 0.06 Å.[1,2a] The cations for these structures range from electrostatically bonded Tl^+ [6] to noncoordinating, sterically encumbering cations such as $[Fe(C_5H_4)_2C_3H_6]^+$.[7]

The solution behavior of $[TCNE]_2^{2-}$, however, is less well-established, and there are even conflicting reports about the existence of $[TCNE]_2^{\bullet-}$ in solution. The initial evidence of an interaction between TCNE and $[TCNE]^{\bullet-}$ putatively forming $[TCNE]_2^{\bullet-}$ in solution[8,9a] was withdrawn by an author;[9b] however, an EPR measured rate of electron exchange between TCNE and $[TCNE]^{\bullet-}$ of order 10^{-9} M^{-1} s^{-1} was reported.[9c] Recently, a more detailed reinvestigation revealed an absorption at 7250 cm^{-1} (1380 nm; 0.90 eV) [ϵ = 1000 cm^{-1} M^{-1}] in MeCN that was attributed to $[TCNE]_2^{\bullet-}$. But it was later found that this species has a TCNE + $[TCNE]^{\bullet-}$ = $[TCNE]_2^{\bullet-}$ equilibrium constant of 0.6 M^{-1}; hence, $[TCNE]_2^{\bullet-}$ prefers to dissociate.[10]

Experimental studies[1b,9b,d,11] indicate the existence of a $2[TCNE]^{\bullet-} \leftrightarrows [TCNE]_2^{2-}$ equilibrium in solution. Dissolution of purple crystals possessing $[TCNE]_2^{2-}$ in the 1 mM range formed yellow [23,375 cm^{-1} (428 nm, 2.90 eV)] solutions of $[TCNE]^{\bullet-}$.[1b] However, in accord with Le Chatalier's principle, upon cooling the equilibrium shifts toward formation of $[TCNE]_2^{2-}$, and this enabled the determination of the electronic absorption spectrum of red $[TCNE]_2^{2-}$ [18,940 cm^{-1} (528 nm, 2.35 eV)] in solution. The dimerization is reversible, and Kochi and co-workers determined the equilibrium constant to be ∼7 × 10^{-4} mol^{-1} at 298 K in CH_2Cl_2,[11] in accord with its rapid dissociation under ambient conditions. Their UV−vis and EPR study of this equilibrium as a function of temperature in dichloromethane identified an ΔS of −41 eu and enthalpy of dissociation (ΔH, or bond dissociation energy) of −36.8 ± 4 kJ/mol (−8.8 ± 1 kcal/mol) obtained from UV−vis measurements. Similar values of ΔS = −36 eu and ΔH = −33.1 kJ/mol (−7.9 kcal/mol) were obtained from the EPR measurements. These values are in good agreement with −33 kJ/mol (−8 kcal/mol) reported by Chang in 1970.[9d] These thermodynamic parameters are unaffected by the size or nature of the counterion (Na^+ versus Et_4N^+); hence, the dimer stability is not signifi-

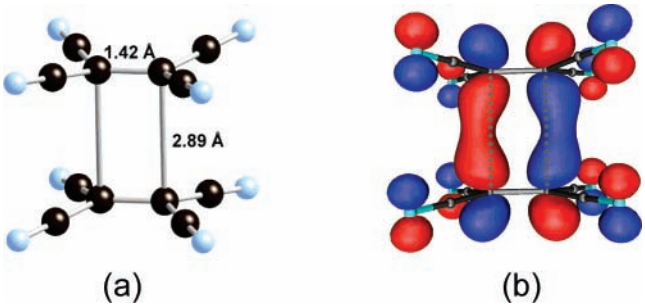

Figure 1. (a) Structure of the π-$[TCNE]_2^{2-}$ dimers; (b) bonding 2e−4c b_{2u} HOMO of the π-$[TCNE]_2^{2-}$ dimer.[1,2a]

[†] Universitat de Barcelona.
[‡] University of Utah.

10.1021/jp073188i CCC: $37.00
Published on Web 07/12/2007

cantly dependent on the counterion.[11] However, their thermodynamic properties are strongly affected by the solvent, although these changes occur without any detectable effect on the UV−vis properties (and consequently the structure) of the π-$[TCNE]_2^{2-}$ dimers.

These π-$[TCNE]_2^{2-}$ dimers are diamagnetic. They also have electronic transitions substantially different from those of the $[TCNE]^{\bullet-}$ monomers.[1b] Furthermore, the dimer characteristic bands are slightly blue-shifted in solution compared to those found in the solid. This suggests that the structure of the $[TCNE]_2^{2-}$ dimers in solution is similar to that found in the solid (an intradimer separation of 3.05 Å is estimated for the dimers found in solution,[11] slightly above the 2.89 Å mean intradimer separation in crystals[1,2a,3]).

Experimental data provides evidence that π-$[TCNE]_2^{2-}$ dimers exist in solution at low temperature. However, (a) the structure of the aggregates, (b) the driving force behind their stability, and (c) an understanding of their electronic spectra remain pending. While experimentally these dimers in solution have an interaction enthalpy of −33.1 kJ/mol, computationally an isolated D_{2h} π-$[TCNE]_2^{2-}$ with an intradimer separation of 3.05 Å is energetically unstable against its dissociation into its monomers by 59.8 kcal/mol (250 kJ/mol) at the B3LYP/6-31+G(d) level, and by 37.7 kcal/mol (158 kJ/mol) at the MCQDPT/CASSCF(2,2) level using the 6-31+G(d) wavefunction (the MCQDPT/CASSCF(2,2) is a high-level multiconfigurational perturbative calculation, similar to a CASPT2 calculation, which properly includes the dispersion component).

Herein, we computationally investigate the structure and stability of the dichloromethane solvated π-$[TCNE]_2^{2-}$ dimers using the B3LYP density functional, CASSCF(2,2), and MCQDPT/CASSCF(2,2) calculations. The origin of the stability of the π-$[TCNE]_2^{2-}$ dimers in solution is identified as the $[TCNE]^{\bullet-}$−solvent interactions, which overcompensate for the $[TCNE]^{\bullet-}\cdots[TCNE]^{\bullet-}$ repulsion. This is computationally demonstrated for $[TCNE]_2^{2-}(solvent)_4$ aggregates, which have minimum energy structures that are energetically stable against their dissociation into its components. Their electronic properties are in agreement with all available experimental data of for the $[TCNE]_2^{2-}$ dimers in solution. They also have an optimum geometry similar to that found in crystals, in accord with the similarity in the experimental properties of the $[TCNE]_2^{2-}$ dimers found in solution and in crystals.

Results and Discussion

1. Models for the Study of the Reversible Association of $[TCNE]^{\bullet-}$ in Solution. The interaction energy curve as a function of the shortest interfragment C···C distance for an isolated D_{2h} π-$[TCNE]_2^{2-}$ dimer computed at the UB3LYP/6-31+G(d) level is presented in Figure 2a. The curve is energetically destabilizing everywhere and shows no minimum at any distance.[12] Despite the energetic instability of the isolated π-$[TCNE]_2^{2-}$ dimers, their existence in ionic crystals was explained[1] by the sum of the $[TCNE]^{\bullet-}\cdots$cation electrostatic interactions exceeding the sum of the $[TCNE]^{\bullet-}$−$[TCNE]^{\bullet-}$ and cation···cation repulsions (Figure 2b). The presence of such energetic overcompensation was computationally demonstrated by the existence of minimum energy $(cation)_2[TCNE]_2$ aggregates.[1,13] For instance, $K_2[TCNE]_2$ aggregates have an energetic stability for their dissociation into its four fragments of −158 kcal/mol (655 kJ/mol) at the UHF/6-31+G(2d,2p) level (similar values were found using other methods and basis sets). Their fully optimized geometry is of D_{2h} symmetry (not imposed during the optimization), and the net charge (obtained from a Mulliken population analysis) on the K^+ atoms is 0.89 e^-. Therefore, $K_2[TCNE]_2$ aggregates are an example of a $(cation)_2$-$[TCNE]_2$ aggregate. Although the electrostatic component is the most relevant to explain the stability of $K_2[TCNE]_2$ and other similar $(cation)_2[TCNE]_2$ aggregates, the dispersion interaction acting between the two $[TCNE]^{\bullet-}$ anions also contributes to the energetic stability of these aggregates.[2c,13] However, the $(cation)_2[TCNE]_2$ aggregate is energetically stable even when the anion−anion dispersion interactions are ignored (as in Hartree−Fock calculations). Thus, the electrostatic interactions are the main driving force behind the existence of these aggregates.

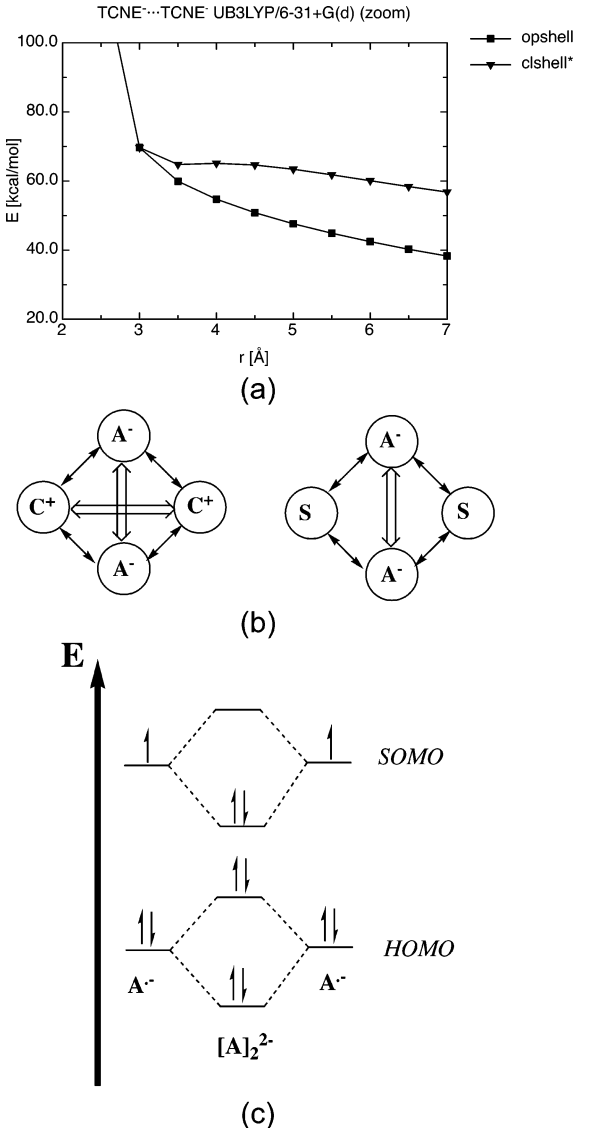

Figure 2. (a) Interaction energy curve for the interaction of two isolated $[TCNE]^{\bullet-}$ monomers computed at the UB3LYP/6-31+G(d) and RB3LYP/6-31+G(d) levels (■ and ▼, respectively; the two monomers are placed in a D_{2h} symmetry). (b) Scheme of an $(anion)_2(cation)_2$ (left: A = anion, C = cation) and an $(anion)_2(solvent)_2$ (right: A = anion, S = solvent) model (wide and thin arrows represent attractive and repulsive interactions). (c) Orbital diagram of the $(anion)_2(cation)_2$ and $(anion)_2(solvent)_2$ in the region of the SOMO of the monomers (a bonding, shown in Figure 1, and an antibonding dimer orbital are formed). The occupation is that for a closed-shell singlet.

The sub van der Waals distance between the anions in these stable $(cation)_2[TCNE]_2$ aggregates enables a non-negligible overlap of the two $[TCNE]^{\bullet-}$ SOMO orbitals. This overlap generates bonding and antibonding combinations of the two SOMOs (Figure 2) that are similar to that found when two

energetically stable monomers interact. As a result, π-$[TCNE]_2^{2-}$ dimers have the same bonding properties associated with covalent C−C bonds, except that their intrinsic stability, i.e., the existence of π-$[TCNE]_2^{2-}$ dimers, does not originate from the stability of the $[TCNE]^-\cdots[TCNE]^-$ as in short distance C−C bonds, but from the $[TCNE]^-\cdots$cation interactions. Hence, they are long, 2-electron/4-center C−C bonds.

The thermodynamic properties of the dissolved π-$[TCNE]_2^{2-}$ dimers do not depend appreciably on the counterion. Along with entropic considerations, it suggests that the presence of $(cation)_2[TCNE]_2$ aggregates is unlikely in solution. Thus, attractive interactions, different from the cation···anion interactions, and capable of compensating the anion···anion repulsion, need to be identified.

The strongest attractive interactions present in $[TCNE]^{\bullet-}$ solutions, besides the cation···anion interactions, are the anion···solvent interactions. Being of the charge-dipole type, the anion···solvent interactions are a lot weaker than the cation···anion interactions (which are of the charge−charge type).[14] However, they were found to be strong enough to explain the formation in solution of energetically stable $(cation)_2(solvent)_n$ aggregates that possess short-distance Au···Au and Ag···Ag interactions between cations.[15] This suggests that the $[TCNE]^{\bullet-}\cdots$solvent interactions could also energetically stablilize $[TCNE]_2^{2-}(solvent)_n$ aggregates having short-distance $[TCNE]^{\bullet-}\cdots[TCNE]^{\bullet-}$ interactions. Such an interanion short distance would allow the two $[TCNE]^{\bullet-}$ SOMO orbitals to overlap, thus generating the same orbital diagram found for $(cation)_2[TCNE]_2^{2-}$ aggregates (see Figure 2c). Consequently, stable $[TCNE]_2^{2-}(solvent)_n$ and $(cation)_2[TCNE]_2$ aggregates should exhibit similar UV−vis and magnetic properties, probably slightly energetically shifted because the optimum $[TCNE]^{\bullet-}\cdots[TCNE]^{\bullet-}$ distance in both aggregates will differ. The reversibility of the $2[TCNE]^{\bullet-} \leftrightarrows [TCNE]_2^{2-}$ equilibrium in solution suggests a small energy difference between the stability of the $[TCNE]_2^{2-}(solvent)_n$ and $(2[TCNE]^{\bullet-})(solvent)_n$ aggregates, which should be within the range of the thermal energy at room temperature. Hereafter, we computationally evaluate the validity of these concepts for dichloromethane solutions, as the most detailed experimental results were reported for this solvent.

2. Strength and Directionality of the $[TCNE]^{\bullet-}\cdots$Solvent Interactions. In order to find the most stable geometrical conformations of the $[TCNE]_2^{2-}-(solvent)_n$ aggregates, one has first to determine the most stable orientations of the $[TCNE]^{\bullet-}\cdots CH_2Cl_2$ interactions, a prototype of weak $[TCNE]^{\bullet-}\cdots$solvent interactions.

Using the optimum MP2/6-31+G(d) geometry of the $[TCNE]^{\bullet-}$ and CH_2Cl_2 fragments, the BSSE-corrected[16−19] interaction energy (Figures 3 and 4) was computed at the MP2/6-31+G(d) level for the most representative $C-H\cdots[TCNE]^{\bullet-}$ and $C-Cl\cdots[TCNE]^{\bullet-}$ orientations of the $[TCNE]^{\bullet-}\cdots CH_2Cl_2$ complex. In the first type of orientation (Figure 3b,c), one of the two C−H groups points toward the $[TCNE]^{\bullet-}$ anion. In the second type of orientation (Figure 4b,c), one of the C−Cl groups points toward the anion. All the $C-H\cdots[TCNE]^{\bullet-}$ curves (Figure 3a) are energetically attractive. The most stable one, with a BSSE-corrected interaction energy of −6 kcal/mol (−25 kJ/mol), is where the C−H group points collinearly toward the CN groups, within the $[TCNE]^{\bullet-}$ plane. On the other hand, the BSSE-corrected $C-Cl\cdots[TCNE]^{\bullet-}$ curves (Figure 4a) are in many cases repulsive, and only in few cases is a minimum found. But when such a minimum is found, it is only marginally stable or metastable (its energy is higher than the energy of the dissociated fragments, and a small barrier prevents its dissociation). Therefore, only the $C-H\cdots[TCNE]^{\bullet-}$ orientations 2 and 4 are important for the most stable arrangements of the stable $[TCNE]_2^{2-}(solvent)_n$ aggregates.

3. Structure of the Most Stable $[TCNE]_2^{2-}(solvent)_4$ Aggregates. Using the aforementioned information, the smallest energetically stable $[TCNE]_2^{2-}(solvent)_n$ aggregate, i.e., n, was searched. Qualitative considerations suggested that the optimum energy will be obtained for a $[TCNE]_2^{2-}(CH_2Cl_2)_4$ aggregate where its four solvent molecules are placed in between the two $[TCNE]^{\bullet-}$ radical-anions allowing each solvent to make two simultaneous $C-H\cdots[TCNE]^{\bullet-}$ contacts. This would allow eight $[TCNE]^{\bullet-}\cdots(CH_2Cl_2)$ interactions and contribute ∼48 kcal/mol (∼200 kJ/mol), without considering cooperative effects. This attractive energy would exceed the $[TCNE]^{\bullet-}-[TCNE]^{\bullet-}$ repulsion at 3.05 Å, which is 37.7 kcal/mol, or 157.7 kJ/mol, according to a MCQDPT/CASSCF(2,2) calculation, using the 6-31+G(d) basis set.

To confirm that stable $[TCNE]_2^{2-}(CH_2Cl_2)_4$ aggregates are stable, (a) these aggregates should be persistent species and have stable minimum energy structures and (b) the two $[TCNE]^{\bullet-}$ anions should be at a short enough distance that their two SOMO orbitals can overlap. In order to evaluate if they fulfill the minimum energy condition, a full geometry optimization of the $[TCNE]_2^{2-}(CH_2Cl_2)_4$ aggregates was performed at the RB3LYP/6-31+G(d) and UB3LYP/6-31+G(d) levels. The RB3LYP calculations find a closed-shell singlet ground state for two doublets placed at 3.05 Å. However, the singlet could also be open-shell, a state that in many cases can only be described with UB3LYP (in some cases the broken-symmetry approach[20] is required to describe an open-shell singlet at the UB3LYP level, but this is not the case in this aggregate). For completeness, the open-shell triplet state at the UB3LYP level was also computed.

The optimum geometry for the closed- and open-shell singlets and the triplet are shown in Figure 5 (although not imposed during the optimization, the fully optimized structures present small deviations from a D_{2h} symmetry). At its optimum geometry, the closed-shell singlet has an occupation of 2.0, 2.0, 0.0, and 0.0 for the four orbitals closest to the HOMO, while at the UB3LYP level the occupation for these orbitals is 2.0, 1.62, 0.38, and 0.00. At the optimum open-shell singlet geometry the UB3LYP wavefunction has an occupation of is 2.0, 1.0, 1.0, and 0.0. The UB3LYP values at the closed- and open-shell optimum geometries are nearly identical to those obtained by doing CASSCF(2,2) calculations at these geometries: 2.0, 1.62, 0.38, and 0.0, at the optimum closed-shell geometry; 2.0, 1.02, 0.98, and 0.0 at the optimum open-shell geometry). Thus, we can conclude that the UB3LYP and RB3LYP methods are describing two different electronic structures and that the RB3LYP wavefunction is purely monodeterminantal while the UB3LYP is multideterminantal. The minimum energy nature of all geometries shown in Figure 5 was confirmed by a vibrational analysis (see the Supporting Information). Although their geometries are similar, the shortest interanion C···C distance differs: 3.033 Å in the closed-shell singlet, 5.227 Å in the open-shell singlet, and 5.232 Å in the triplet. Therefore, only in the closed-shell singlet are the two anions close enough to allow a non-negligible overlap of their SOMOs. Another concern of these B3LYP calculations is that the three minima have positive formation energy, suggesting that they are computationally metastable, as demonstrated in Figure S1, as already found in $(cation)_2[TCNE]_2$ aggregates.[13] This metastability could originate in the wrong estimate that the B3LYP functional makes of the dispersion component. This possibility

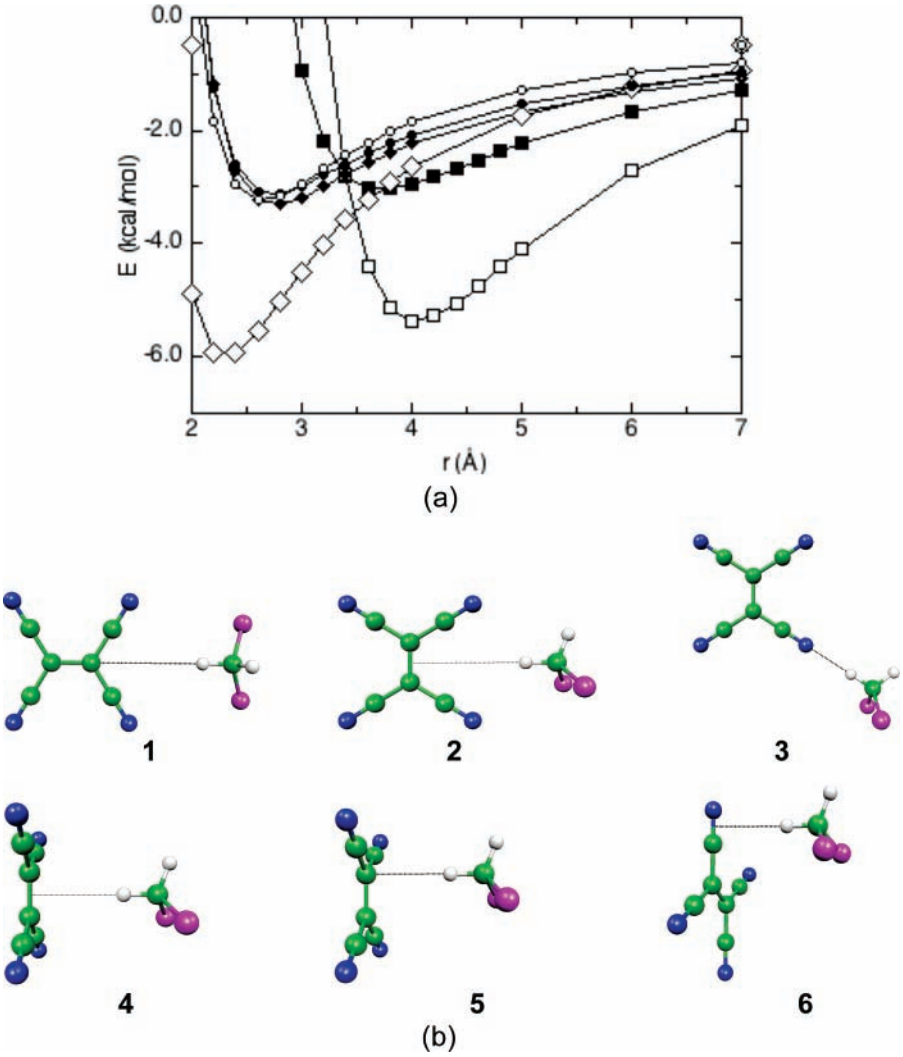

Figure 3. (a) Variation of the $[TCNE]^{\bullet-}\cdots CH_2Cl_2$ interaction energy (E) with the shortest H···$[TCNE]^{\bullet-}$ distance (r, depicted in Figure 3b) when the solvent is oriented with its C−H group pointing toward the $[TCNE]^{\bullet-}$ anion. The results were computed at the UMP2/6-31+G(d) level, and the orientations are identified as follows: 1 = ■, 2 = □, 3 = ◇, 4 = ◆, 5 = ●, and 6 = ○. (b) Geometry of the orientations for which the interaction energy has been computed, indicating the shortest H···$[TCNE]^{\bullet-}$ distance.

can be checked by doing MCQDPT/CASSCF(2,2) calculations on the $[TCNE]_2^{2-}(CH_2Cl_2)_4$ aggregates.

The shape of the potential energy curves for these closed-shell and open-shell singlet states as a function of the interanion C−C distance was also evaluated to identify if they interconvert above a given distance. The BSSE-corrected and uncorrected curves (computed at the RB3LYP/6-31+G(d) level for the closed-shell singlet, and at the UB3LYP/6-31+G(d) level for the open-shell singlet) are shown in Figure 6. They show that, irrespectively of the BSSE error, the closed-shell singlet curve does not convert into the open-shell singlet curve at large distances. However, the two curves overlap at short distances; thus, the closed-shell minimum transforms into the open-shell minimum when the double occupancy restriction of the RB3LYP calculation is lifted. Thus, the only real minimum at the B3LYP level is the open-shell (paramagnetic[21]) ground state. This result contradicts the experimental observation that the π-$[TCNE]_2^{2-}$ dimers have a closed-shell singlet (diamagnetic-like) ground state. Note that the same erroneous result was found in the $(cation)_2[TCNE]_2$ aggregate using the B3LYP functional. However, this error was corrected when the dispersion energy was properly accounted for by MCQDPT/CASSCF(2,2) calculations.[13]

In order to identify if the computationally predicted erroneous paramagnetic ground state could be corrected by including the effect of the remaining solvent molecules, the bulk solvent effect was evaluated, using the CPCM continuous model,[22] for the closed- and open-shell singlet curves (Figure 7). However, the new curves show that the bulk solvent effects are similar in both cases; thus, the open-shell curve remains as the most stable one.

The CASSCF(2,2) and MCQDPT/CASSCF(2,2)[23] curves for the closed- and open-shell singlet states of the $[TCNE]_2^{2-}(CH_2Cl_2)_4$ aggregate (Figure 8) were then computed using in both cases the 6-31+G(d) basis set. The closed-shell curves were computed using the optimum geometries from the RB3LYP calculations, while the open-shell curves were computed using the optimum UB3LYP/6-31+G(d) geometry. The CASSCF(2,2) curve (Figure 8a) has only one minimum of the open-shell singlet type. However, the MCQDPT/CASSCF(2,2) curve (Figure 8b) has its only minimum at 2.75 Å, and is closed-shell. Thus, when the dispersion component is properly included (MCQDPT/CASSCF(2,2) calculations), the $[TCNE]_2^{2-}(CH_2Cl_2)_4$ aggregate has a diamagnetic-like closed-singlet ground state, in good agreement with the experimental nature of the $[TCNE]^{\bullet-}$ dichloromethane solutions at low temperature. The MCQDPT/

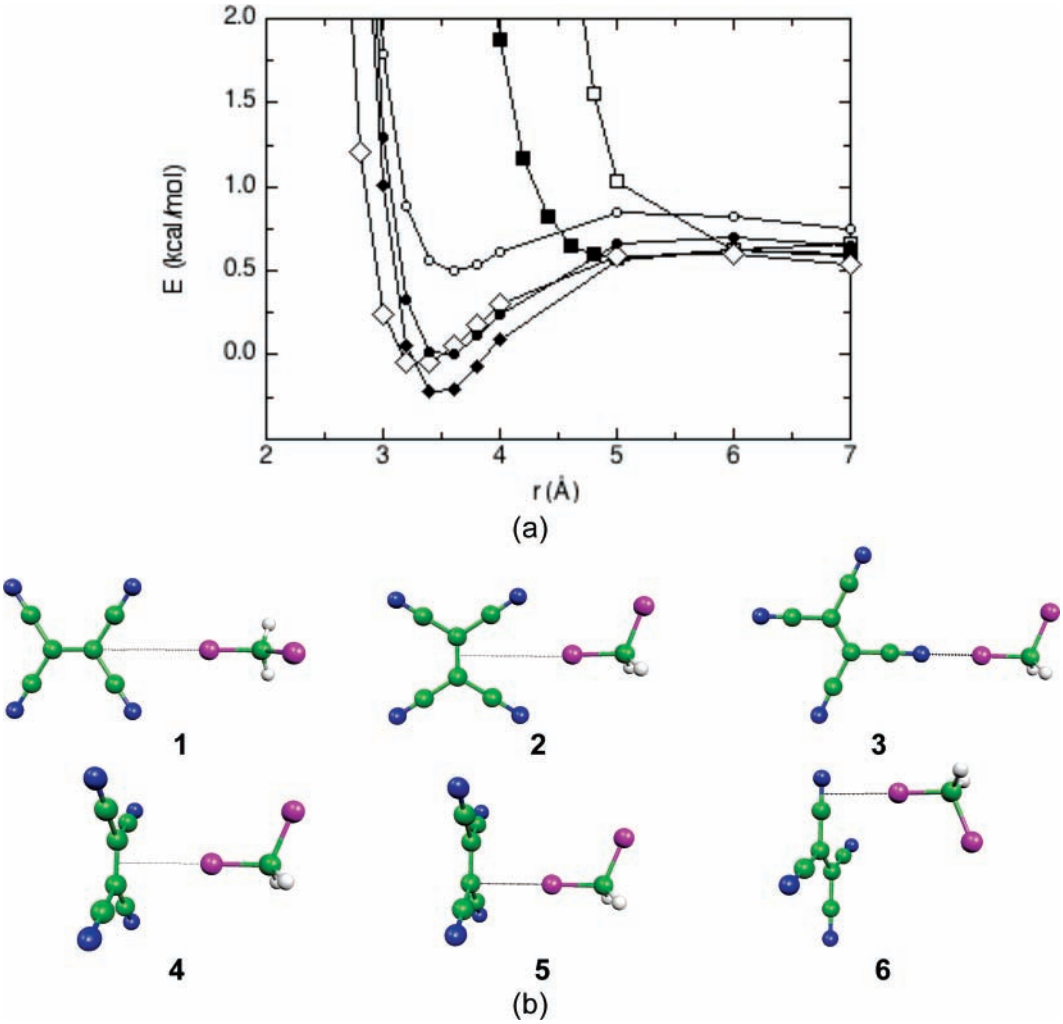

Figure 4. (a) Variation of the $[TCNE]^{\bullet-}\cdots CH_2Cl_2$ interaction energy (E) with the shortest $Cl\cdots[TCNE]^{\bullet-}$ distance (r, depicted in Figure 4b) when the solvent is oriented with its C−Cl group pointing toward the $[TCNE]^{\bullet-}$ anion. The results were computed at the UMP2/6-31+G(d) level, and the orientations are identified as follows: 1 = ■, 2 = □, 3 = ◇, 4 = ◆, 5 = ●, and 6 = ○. (b) Geometry of the orientations for which the interaction energy has been computed, indicating the shortest $Cl\cdots[TCNE]^{\bullet-}$ distance.

CASSCF(2,2) minimum is also energetically stable, by −24.0 kcal/mol (101 kJ/mol). This agrees with the experimental data, as the $[TCNE]_2^{2-}$ dimers only dissociate when the temperature is increased. The remaining solvent molecules that form the bulk also provide an extra stabilization for these aggregates, although this could not be evaluated at the MCQDPT/CASSCF(2,2) level. Note that this theoretical interaction energy is slightly stronger than the experimental ΔH for the 2 $[TCNE]^{\bullet-} \leftrightarrows [TCNE]_2^{2-}$ process in solution. This is expected because the theoretical interaction energy refers to the energy to create the cluster from its six fragments, while the experimental energy refers to the difference in energy between a $[TCNE]_2^{2-}$ aggregate and two solvent-separated $[TCNE]^{\bullet-}$ monomers placed in a dichloromethane solution. In summary, at the MCQDPT/CASSCF(2,2) level the $[TCNE]_2^{2-}(CH_2Cl_2)_4$ aggregates become persistent, energetically stable species with a short interanion C···C distance that allow the overlap of the SOMO orbitals of the anions.

Analysis of the electronic properties of the persistent $[TCNE]_2^{2-}(CH_2Cl_2)_4$ aggregates was done via the similarities with the $(cation)_2[TCNE]_2^{2-}$ UV−vis spectra. The $[TCNE]_2^{2-}(CH_2Cl_2)_4$ electronic structure can be rationalized using Figure 2c. The three states studied herein have the same bonding and antibonding orbitals at the B3LYP level (Figure S2) that result from the bonding and antibonding combination of the two $[TCNE]^{\bullet-}$ π^* SOMO orbitals. These three states differ only in the occupation of the bonding and antibonding orbitals. (Closed-shell singlet: two electrons in the bonding combination and none in the antibonding. Open-shell singlet and triplet states: one electron in each of these two orbitals.) Therefore, the MO diagram of the $[TCNE]_2^{2-}(CH_2Cl_2)_4$ aggregate is identical in the HOMO and LUMO to that reported for $(cation)_2[TCNE]_2$ aggregates.[1] This explains the similarity in UV−vis and magnetic properties of the $[TCNE]_2^{2-}$ dimers found in solution and in crystals.

Finally, an AIM analysis[24] of the bonds that appear in the $[TCNE]_2^{2-}(CH_2Cl_2)_4$ aggregate was performed. The (3,−1) bond critical points were also located for the three states at their optimum geometry (Figure 5). In all cases two interanion C···C bond critical points are found (Figure 5). In good agreement with a longer C···C distance in the open-shell singlet and triplet states, the critical points in these two states have a much smaller computed density (2.06×10^{-4} a.u.) than the 1.35×10^{-2} a.u. obtained in the closed-shell singlet. These densities can be compared with those computed for the C−H···N bond critical point in the three states, $\sim 1.16 \times 10^{-2}$ a.u. It is also worth pointing that all the C···C (3,−1) bond critical points and all C−H···N bond critical points have a positive Laplacian[25] (7.97×10^{-4} a.u. in the C···C case, and 3.58×10^{-2} a.u. in the C−H···N case). These results are expected for the closed-

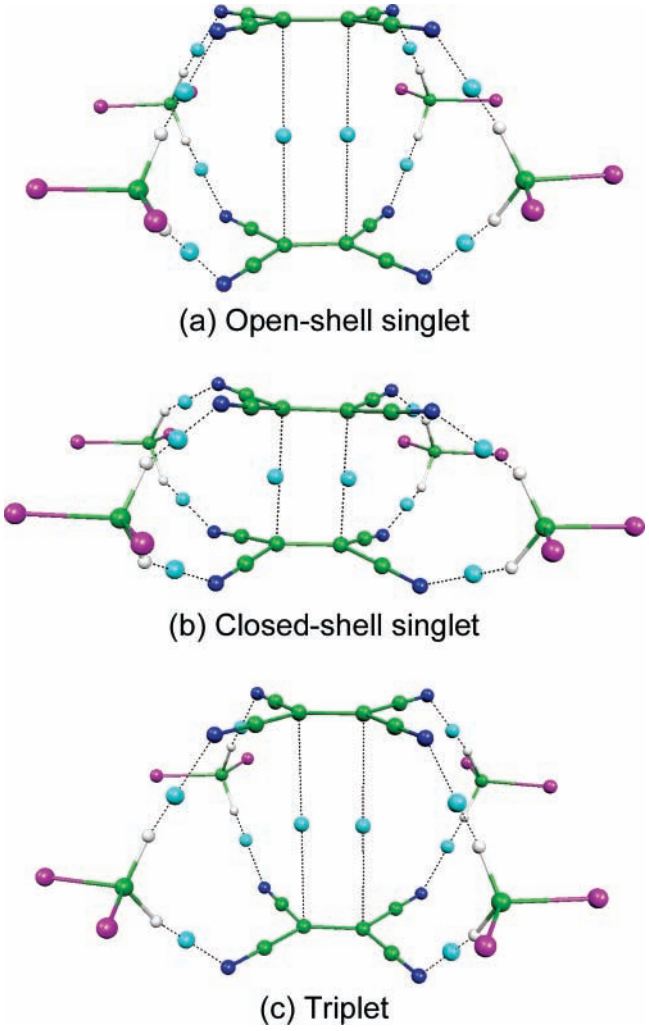

Figure 5. Optimum geometry of the $[TCNE]_2^{2-}(CH_2Cl_2)_4$ aggregate: (a) for the open-shell state computed at the UB3LYP/6-31+G(d) level (the shortest C−C distance between the anions is 5.227 Å, while the shortest C−H···N($TCNE^-$) distance is 2.409 Å); (b) for the closed-shell state computed at the RB3LYP/6-31+G(d) level (the shortest C−C distance between the anions is 3.033 Å, while the shortest C−H···N($TCNE^-$) distance is 2.381 Å); (c) for the open-shell state computed at the UB3LYP/6-31+G(d) level (the shortest C−C distance between the anions is 5.232 Å, while the shortest C−H···N($TCNE^-$) distance is 2.409 Å). In the three cases the position of the (3,−1) bond critical points is also shown (in light blue), indicating in broken lines the bonded atoms (see text). Although no symmetry was imposed during the optimization, all aggregates present a small deviation from a D_{2h} symmetry.

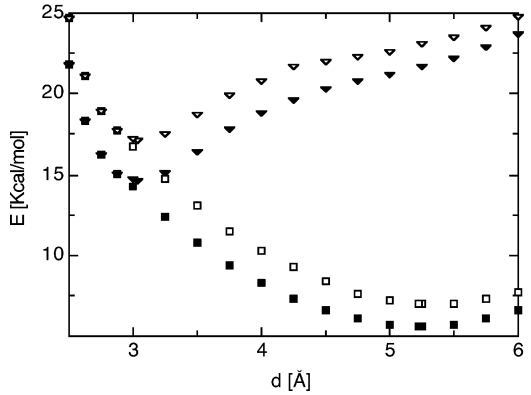

Figure 6. Variation of the interaction energy (*E*) of the closed- and open-shell singlet of the $[TCNE]_2^{2-}(CH_2Cl_2)_4$ aggregate with the shortest interanion distance (*d*). Two curves are shown for the closed-shell singlet: the BSSE-corrected corrected (▽) and the BSSE-uncorrected (▼) curves. Similarly, two curves are given for the open-shell singlet: the BSSE-corrected corrected (□) and the BSSE-uncorrected (■) curves. The zero of energy in these curves corresponds to the dissociation into its six fragments at their optimum UB3LYP geometry.

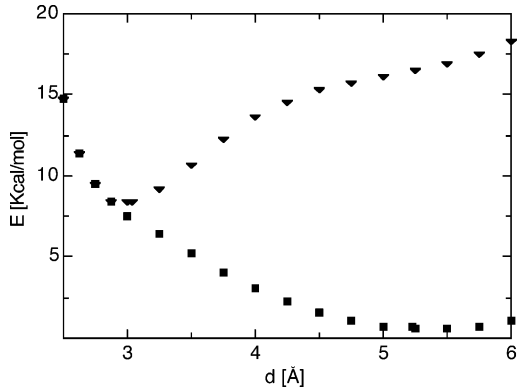

Figure 7. Variation of the solvent-corrected interaction energy (*E*) of the closed- and open-shell singlet of the $[TCNE]_2^{2-}(CH_2Cl_2)_4$ aggregate with the shortest interanion distance (*d*). The closed-shell singlet curve computed at the RB3LYP level is indicated by ▼, while that for the open-shell singlet is indicated by ■. In both cases the solvent effect was computed using the CPCM method. The zero of energy in these curves corresponds to the dissociation into its six fragments at their optimum UB3LYP geometry.

shell singlet state. However, the presence of critical points for the long C···C separations in the triplet and open-shell singlet states is surprising, as no long C−C bonds can be formed in these states. These results suggest that in these cases the presence of a (3,−1) bond critical point is *not a sufficient* condition for the existence of a bond, and that other conditions are also required (for instance, the energetic stability of the interaction, as required in Pauling's definition of a bond[26]). Other examples where the presence of a (3,−1) bond critical point is *not a sufficient* condition for the existence of a bond have been reported, but they are still the subject of discussion.[27] As no overcrowding or steric factors are relevant in this aggregate, it is a clear example that the existence of a (3,−1) critical point is not a sufficient condition for the presence of a bond. It is also worth mentioning that a similar conclusion was reached when analyzing the (3,−1) bond critical points found in the $[TCNE]_2^{2-}(cation)_2$ aggregate. Further investigation of the properties of these (3,−1) bond critical points is currently under further study and will be the subject of a further report.

Conclusions

The existence of a minimum-energy $[TCNE]_2^{2-}(CH_2Cl_2)_4$ aggregate, where short distance $[TCNE]_2^{2-}$ dimers are observed, is computationally identified. These dimers can be found at the B3LYP level, but not at the CASSCF(2,2) level. However, only upon properly taking into account the dispersion energetic component (as in MCQDPT/CASSCF(2,2) calculations) are these dimers energetically more stable than their fragments. The only minimum found in the potential energy curve at the MCQDPT/CASSCF(2,2) level has its two $[TCNE]^{\bullet-}$ fragments separated by 2.75 Å, a distance where the SOMOs of these two anions can overlap and have all the features of a long, 2-electron/4-center C−C bond. They are observed at low temperature and under the proper concentration conditions. Therefore, these $[TCNE]_2^{2-}(CH_2Cl_2)_4$ aggregates can explain all the experimentally known properties of the $[TCNE]^{\bullet-}$ salts in dichloromethane.

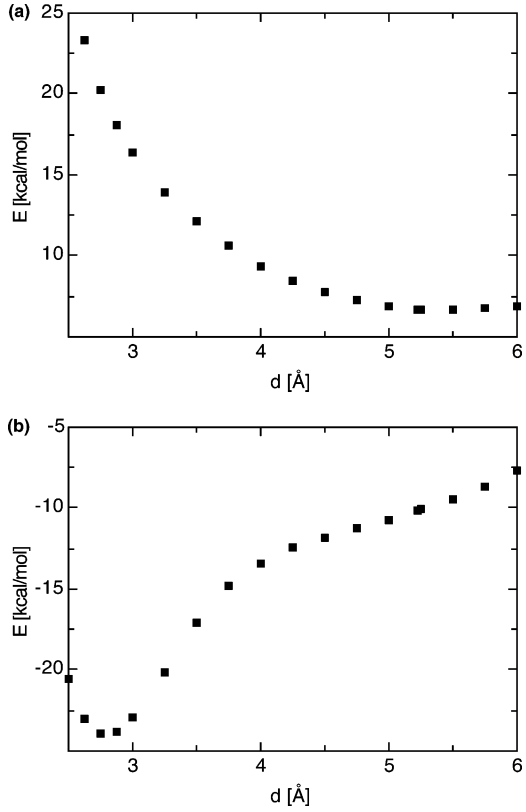

Figure 8. Variation of the interaction energy (E) computed for the $[TCNE]_2^{2-}(CH_2Cl_2)_4$ aggregate with the shortest interanion distance (d). Top, a: CASSCF(2,2) curve. Bottom, b: MCQDPT/CASSCF(2,2) curve. Note the effect of dispersion (not included in CASSCF(2,2) calculations) in changing the minimum of the curve. The zero of energy in these curves corresponds to the dissociation into its six fragments at their optimum UB3LYP geometry.

It is also worth mentioning that the existence of $[TCNE]_2^{2-}(CH_2Cl_2)_4$ aggregates at low enough temperature can have some important implications for the growth of $[TCNE]^{\bullet-}$-containing crystals, as it is likely that the crystal will show some preference to preserve the $[TCNE]_2^{2-}$ dimers when they are already in solution. This is relevant when using inert solvents that have stronger interactions with the anions (any with a dielectric constant larger than that for dichloromethane[28]) as then the stability of the $[TCNE]_2^{2-}(solvent)_4$ aggregates is remarkably increased (the reason being that the $[TCNE]^{\bullet-}\cdots$solvent interactions are the driving force behind the existence of these aggregates).

Computational Details

All calculations were done using the 6-31+G+(d) basis set.[29] The B3LYP calculations[30] were done using the implementation of this functional found in Gaussian-03,[31] while the CASSCF-(2,2)[32] and MCQDPT/CASSCF(2,2) calculations[33] were done using GAMESS-05[34] on the optimum B3LYP geometry. The solvent effects, taken into account by means of the continuous CPCM,[20] were computed on the B3LYP wavefunction using Gaussian-03.[28]

Acknowledgment. The Spanish team was supported by the Spanish Science and Education Ministery (Projects BQU2002-04587-C02-02 and UNBA05-33-001, and a Ph.D. grant to I.G.-Y.) and the CIRIT (Projects 2001SGR-0044 and 2005-PEIR-0051/69). Computer time was also provided by CESCA and BSC. J.S.M. was supported by the NSF (Grant No. 0553573) and the DOE (Grant No. DE FG 03-93ER45504). This paper is dedicated to the memory of Professor Lorenzo Pueyo.

Supporting Information Available: Complete ref 31; optimum geometry, total energy, lowest vibrational frequencies, atomic spin population, and atomic charge population of the $(TCNE)_2(CH_2Cl_2)_4$ aggregates, in their closed- and open-shell singlet and triplet states; variation of the interaction energy of the $[TCNE]_2^{2-}(CH_2Cl_2)_4$ aggregate with the distance between the two anions; shape of the two SOMOs of the open-shell singlet and triplet states, and of the HOMO and LUMO of the closed-shell singlet state. This material is available free of charge via the Internet at http://pubs.acs.org.

References and Notes

(1) (a) Novoa, J. J.; Lafuente, P.; Del Sesto, R. E.; Miller, J. S. *Angew. Chem., Int. Ed.* **2001**, *40*, 2540. (b) Del Sesto, R. E.; Miller, J. S.; Novoa, J. J.; Lafuente, P. *Chem. Eur. J.* **2002**, *8*, 4894. (c) Novoa, J. J.; Lafuente, P.; Del Sesto, R. E.; Miller, J. S. *CrystEngComm* **2002**, *4*, 373.

(2) (a) Lu, J.-M.; Rosokha, S. V.; Kochi, J. K. *J. Am. Chem. Soc.* **2003**, *125*, 12161. (b) Jakowski, J.; Simons, J. *J. Am. Chem. Soc.* **2003**, *125*, 16089. (c) Jung, Y.; Head-Gordon, M. *Phys. Chem. Chem. Phys.* **2004**, *6*, 2008.

(3) Miller, J. S.; Novoa, J. J. *Acc. Chem. Res.* **2007**, *40*, 189.

(4) Bagnato, J. D.; Shum, W. W.; Strohmeier, M.; Grant, D. M.; Arif, A. M.; Miller, J. S. *Angew. Chem., Int. Ed.* **2006**, *45*, 5326; *Angew. Chem.* **2006**, *118*, 5452.

(5) Goto, G.; Kubo, T.; Yamamoto, K.; Nakazawa, S.; K. Sato, K.; Shiomi, D.; Takui, T.; Kubota, M.; Kobayshai, Y.; Yakusi, K.; Ouyang, J. A. *J. Am. Chem. Soc.* **1999**, *121*, 1619.

(6) Johnson, M. T.; Campana, C. F.; Foxman, B. M.; Desmarais, W.; Vela, M. J.; Miller, J. S. *Eur. J. Chem.* **2000**, *6*, 1805.

(7) Lemervoskii, D. A.; Stukan, R. A.; Tarasevich, B. N.; Slovokhotov, T. L.; Antipin, M. Y.; Kalinin, A. E.; Struchov, Y. T. *Struct. Khim.* **1981**, *7*, 240.

(8) Phillips, W. D.; Powell, J. C. *J. Chem. Phys.* **1960**, *33*, 626; Chang, R. *J. Phys. Chem.* **1970**, *74*, 2029. Chesnut, D. B.; Phillips, W. D. *J. Chem. Phys.* **1961**, *35*, 1002.

(9) (a) Itoh, M. *J. Am. Chem. Soc.* **1970**, *92*, 886. (b) Itoh, M. *Bull. Chem. Soc. Jpn.* **1972**, *45*, 1947. (c) Komarynsky, M. A.; Wahl, A. C. *J. Phys. Chem.* **1975**, *79*, 695. (d) Chang, R. *J. Phys. Chem.* **1970**, *74*, 2029.

(10) Ganesan, V.; Rosokha, S. V.; Kochi, J. *J. Am. Chem. Soc.* **2003**, *125*, 2559.

(11) Lü, J.-M.; Rosokha, S. V.; Kochi, J. *J. Am. Chem. Soc.* **2003**, *125*, 12161.

(12) N*o*tice, however, that when computed at the RHF or RB3LYP levels an unphysical metastable minimum appears ~3.2 Å as a consequence of the double occupancy restriction, although these minima disappear when the double occupancy restriction is released, as in UB3LYP calculations

(13) Garcia-Yoldi, I.; Mota, F.; Novoa, J. J. *J. Comput. Chem.* **2007**, *28*, 326.

(14) Israelachvili, J. *Intermolecular and Surface Forces*, 2nd ed.; Academic Press: Amsterdam, 1992.

(15) Carvajal, M. A.; García-Yoldi, I.; Novoa, J. J. *J. Mol. Struct. (THEOCHEM)* **2005**, *727*, 181. Carvajal, M. A.; Alvarez, S.; Novoa, J. J. *Theor. Chem. Acc.* **2006**, *116*, 472.

(16) BSSE (Basis-set-superposition error) is the error introduced by the use of finite basis sets when computing the interaction energy between two molecules. As originally shown by Boys and Bernandi (ref 17), it can be corrected by using the counterpoise correction. The validity of such correction was questioned by some authors, but is shown to be valid on the basis of analytical (ref 18) and numerical (ref 19) studies when basis sets of good quality are used.

(17) Boys, S. F.; Bernardi, F. *Mol. Phys.* **1970**, *19*, 553.

(18) van Duijneveldt, F. B.; van Duijneveldt-van de Rijdt, J. G. C. M.; van Lenthe, J. H. *Chem. Rev.* **1994**, *94*, 1873.

(19) Novoa, J. J.; Planas, M.; Whangbo, M.-H. *Chem. Phys. Lett.* **1994**, *225*, 240.

(20) Noodleman, L. *J. Chem. Phys.* **1981**, *74*, 5737. Noodleman, L.; Davidson, E. *Chem. Phys.* **1986**, *109*, 131.

(21) At long distance the open-shell singlet and triplet states are nearly degenerate. Thus, the open-shell singlet is one of the two components of a paramagnetic state. If it would not exist and be degenerate, the state would be either ferromagnetic (a triplet) or diamagnetic (a closed-shell singlet).

(22) Barone, V.; Cossi, M. *J. Phys. Chem. A* **1998**, *102*, 1995.

(23) CASSCF(2,2) refers to a CASSCF calculation done using a complete active space built with two electrons and two orbitals. They provide a proper description of the open-shell and closed-shell singlet states at all

distances. MCQDPT/CASSCF(2,2) are quasidegenerate perturbation calculations using as reference the CASSCF(2,2) wavefunction.

(24) Bader, R. F. W. *Atoms in Molecules*; Oxford University Press: Oxford, U.K., 1990.

(25) Sum of the eigenvalues of the second derivative of the electron density at the critical point. Covalent bonds have a negative Laplacian, while van der Waals, ionic bonds, and hydrogen bonds have positive Laplacian.

(26) Pauling, L. *The Nature of the Chemical Bond*, 3rd ed.; Cornell University Press: Ithaca, NY, 1960; p 6.

(27) (a) Cioslowski, J.; Mixon, S. T. *J. Am. Chem. Soc.* **1992**, *114*, 4382. (b) Poater, J.; Solà, M.; Bickelhaupt, F. M. *Chem. Eur. J.* **2006**, *12*, 2889. (c) Matta, C. F.; Hernandez-Trujillo, J.; Tang, T.-H.; Bader, R. F. W. *Chem. Eur. J.* **2003**, *9*, 1940.

(28) The shortest solvent−anion interaction in CH_2Cl_2 solution is of the C-H···anion type, and hydrogen bonds of the C-H···X type are weaker than O−H···X or N-H···X hydrogen bonds, due to the smaller dipole that the C−H bonds present.

(29) Ditchfield, R.; Hehre, W. J.; Pople, J. A. *J. Chem. Phys.* **1971**, *54*, 724.

(30) Becke, A. D. *J. Chem. Phys.* **1993**, *98*, 5648. Lee, C.; Yang, W.; Parr, R. G. *Phys. Rev. B* **1988**, *37*, 785.

(31) Frisch, M. J.; et al. *Gaussian-03*, revision-C.02; Gaussian, Inc.: Wallingford, CT, 2004.

(32) Szabo, A.; Ostlund, N. S. *Modern Quantum Chemistry*; Macmillan: New York, 1982.

(33) The QMCQDPT acronym refers to a second-order Moller−Plesset, multiconfigurational quasidegenerate perturbative theory implemented by Nakano et al. See: Nakano, H.; Nakayama, K.; Hirao, K.; Dupuis, M. *J. Chem. Phys.* **1997**, *106*, 4912.

(34) Schmidt, M. W.; Baldridge, K. K.; Boatz, J. A.; Elbert, S. T.; Gordon, M. S.; Jensen, J. H.; Koseki, S.; Matsunaga, N.; Nguyen, K. A.; Su, S. J.; Windus, T. L.; Dupuis, M.; Montgomery, J. A. *J. Comput. Chem.* **1993**, *14*, 1347.